Guaranteed-passive simulation of an electro-mechanical piano: A port-Hamiltonian approach

Antoine Falaize, Thomas Hélie

GUARANTEED-PASSIVE SIMULATION OF AN ELECTRO-MECHANICAL PIANO: A PORT-HAMILTONIAN APPROACH

Antoine Falaize, *

IRCAM, CNRS (UMR 9912)
Analysis/Synthesis Team
Paris, France
antoine.falaize@ircam.fr

Thomas Hélie,

IRCAM, CNRS (UMR 9912)
Analysis/Synthesis Team
Paris, France
thomas.helie@ircam.fr

ABSTRACT

This paper deals with the time-domain simulation of a simplified electro-mechanical piano. The physical model is composed of a hammer (nonlinear component), a cantilever beam (damped linear resonator) and a pickup (nonlinear transducer). In order to ensure stable simulations, a method is proposed, which preserves passivity, namely, the conservative and dissipative properties of the physical system. This issue is addressed in 3 steps. First, each physical component is described by a passive input-output system, which is recast in the port-Hamiltonian framework. In particular, a passive finite dimensional model of the Euler-Bernoulli beam is derived, based on a standard modal decomposition. Second, these components are connected, providing a nonlinear finite dimensional port-Hamiltonian system. Third, a numerical method is proposed, which preserves the power balance and passivity. Numerical results are presented and analyzed.

1. INTRODUCTION

This paper address the time-domain simulation of a multi-physics musical instrument, namely, an electro-mechanical piano. A particular attention is devoted to preserving the passivity of the original physical system, especially in the discrete-time domain (that is, no energy is artificially created in the numerical system during the simulation). Such an approach has been considered in *e.g.* [1, 2], with an emphasis on numerical issues. In contrast, other methods such as *physically informed sound synthesis* [3, 4], can lead to numerical systems whose stability is difficult to ensure.

Here, we consider the *port-Hamiltonian* approach, introduced in the 1990's [5, 6, 7]. Port-Hamiltonian systems are extensions of classical Hamiltonian systems [8]: they model open dynamical systems made of energy storage components, dissipative components, and some connection ports through which energy can transit. This leads to a state-space representation of multiphysics systems structured according to energy flow, thus encoding the passivity property including for nonlinear cases.

As depicted in figure 1, the model is composed of a hammer $\mathcal{H}$ (nonlinear component with hysteresis), a cantilever beam $\mathcal{B}$ (damped linear infinite dimensional resonator) and a pickup $\mathcal{P}$ (nonlinear mechano-electric transducer). In addition, the pickup is connected to a TLC analog filter (not shown in figure 1). The physical modeling of those elements are available in the literature and are recalled.

This paper is organized as follows. The port-Hamiltonian (pH) framework is recalled in section 2 and we show how this formalism ensures the passivity of the models in continuous time. Section 3 describes the lumped components $\mathcal{H}$, $\mathcal{P}$ and the RLC circuit, and provides their modeling into pH formalism Section 4 is devoted to the pH formulation of the Euler-Bernoulli beam $\mathcal{B}$ through its finite-dimensional approximation, based on a standard modal decomposition. These components are connected in section 5, providing a nonlinear finite-dimensional port-Hamiltonian system. In section 6, a numerical method is proposed, which preserves the power balance and thus the passivity in discrete time. Numerical results are presented and analyzed in section 7.

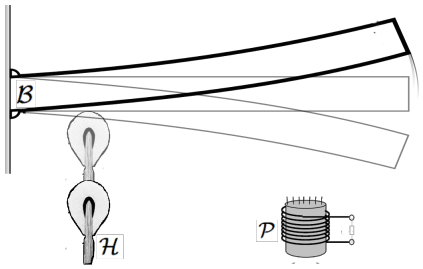

Figure 1: Schematic of the simplified electromechanical piano, with hammer $\mathcal{H}$, beam $\mathcal{B}$ and pickup $\mathcal{P}$.

2. PORT-HAMILTONIAN SYSTEMS

In this section, we introduce the *port-Hamiltonian* (pH) formalism [5, 6, 7] and present an introductory example. It is shown how this structure guarantees the passivity of the model in continuous time.

2.1. Considerations on energy and passivity

Denote $\mathtt{E}(t) \geq 0$ the energy stored in an open physical system. If the system is autonomous and conservative, its time variation $\frac{\mathrm{d}\mathtt{E}}{\mathrm{d}t}(t)$ is zero. If the system is controlled (non-autonomous) and conservative, $\frac{\mathrm{d}\mathtt{E}}{\mathrm{d}t}(t)$ is the power $\mathtt{S}(t)$ received from the sources through the external ports. If the system includes dissipative phenomena with dissipated power $\mathtt{D}(t) \geq 0$, the evolution of energy satisfies the following *power balance*:

$$\frac{\mathrm{d}\mathtt{E}}{\mathrm{d}t}(t) = -\mathtt{D}(t) + \mathtt{S}(t). \tag{1}$$

* The contribution of both authors has been done at IRCAM Laboratory, Paris, within the context of the French National Research Agency sponsored project HAMECMOPSYS. Further information is available at http://www.hamecmopsys.ens2m.fr.

Such systems are passive in the sens that $\frac{\mathrm{dE}}{\mathrm{d}t} \leq \mathtt{S}$. In particular, if the sources are not activated, $\frac{\mathrm{dE}}{\mathrm{d}t} \leq 0$. The dynamic input-to-output behavior of such system is the result of the intricate power exchange between isolated lumped or distributed components. For finite-dimensional systems, those components are sorted as (or can be a combination of): s components that store energy $\mathtt{E} \geq 0$ (moving mass, capacitors), d components that dissipate power $\mathtt{D} \geq 0$ (mechanical damping, transistors), p external ports that convey power $\mathtt{S}$ ($\in \mathbb{R}$) from sources (mechanical loads, 9V batteries) or any external system (active, dissipative or mixed). The behavior of each component is described by a relation between two sets of *power variables*: flows $\mathfrak{f}$ (velocities, currents, variation of magnetic flux) and the associated efforts $\mathfrak{e}$ (forces, voltages, magnetomotive forces). Based on *receiver convention*, the received power is $\mathtt{P} = \mathfrak{f}^\intercal \mathfrak{e}$.

The total stored energy is expressed as a *storage functional* (Hamiltonian) H of an appropriate *state* $\mathbf{x}$. It is built from the sum of the locally stored energies $\mathtt{E} = \mathrm{H}(\mathbf{x}) = \sum_{n=1}^{s} \mathrm{H}_n(\mathbf{x}_n)$. Typically, for a mass m, the state can be the momentum $x = m\frac{\mathrm{d}q}{\mathrm{d}t}$ and the positive definite function is $\mathrm{H}_m(x) = \frac{1}{2m}x^2$. Storage power variables $(\mathfrak{f}_\mathcal{S}, \mathfrak{e}_\mathcal{S})$ are related to the variation of the state $\frac{\mathrm{d}\mathbf{x}}{\mathrm{d}t}$ and the gradient of the storage function $\nabla\mathrm{H}(\mathbf{x})$, the product of which is precisely the *received power*: $\mathfrak{f}_\mathcal{S}^\intercal \mathfrak{e}_\mathcal{S} = \frac{\mathrm{dE}}{\mathrm{d}t} = \nabla\mathrm{H}(\mathbf{x})^\intercal \frac{\mathrm{d}\mathbf{x}}{\mathrm{d}t}$. For the mass, it yields $\mathfrak{f}_m = \frac{\mathrm{d}q}{\mathrm{d}t} = H'_m$ and $\mathfrak{e}_m = m\partial_t^2 q = \frac{\mathrm{d}x}{\mathrm{d}t}$.

The total dissipated power is expressed with respect to an appropriate *dissipation variable* $\mathbf{w}$ and is built from the sum of the locally dissipated powers $\mathtt{D}(t) \equiv \mathtt{D}\big(\mathbf{w}(t)\big) = \sum_{n=1}^{d} \mathtt{D}_n\big(\mathbf{w}_n(t)\big)$. Typically, for a fluid-type damper α, w can be a velocity $w = \frac{\mathrm{d}q}{\mathrm{d}t}$ and $\mathtt{D}_\alpha(w) = \alpha w^2$. As for storage components, a mapping of the dissipative power variables $(\mathfrak{f}_\mathcal{D}, \mathfrak{e}_\mathcal{D})$ is provided, based on the factorization $\mathtt{D}(\mathbf{w}) = \mathbf{w}^\intercal \mathbf{z}(\mathbf{w})$, introducing a *dissipation function* $\mathbf{z}$. For the damper, $\mathfrak{f}_\alpha = \frac{\mathrm{d}q}{\mathrm{d}t}$ and $\mathfrak{e}_\alpha = z_\alpha(w) = \alpha w$.

For an input/output system, we arrange source variables $(\mathfrak{f}_\mathcal{P}, \mathfrak{e}_\mathcal{P})$ in two vectors: one is considered as an *input* $\mathbf{u}$ and the other as the associated *output* $\mathbf{y}$ so that the power received form sources is $\mathtt{S} = \mathfrak{f}_\mathcal{P}^\intercal \mathfrak{e}_\mathcal{P}$.

2.2. State-space representation of port-Hamiltonian systems

The algebraic-differential system of equations that governs a passive system is obtained by applying conservation laws (Newton, Kirchhoff) to the interconnection network. This system can be recast into the *port-Hamiltonian systems* formalism [7, eq 2.53]:

$$\underbrace{\left(\begin{array}{c} \frac{\mathrm{d}\mathbf{x}}{\mathrm{d}t} \\ \hline \mathbf{w} \\ \hline -\mathbf{y} \end{array}\right)}_{\mathbf{a}} = \underbrace{\left(\begin{array}{c|c|c} \mathbf{J_x} & -\mathbf{K} & -\mathbf{G_x} \\ \hline \mathbf{K}^\intercal & \mathbf{J_w} & -\mathbf{G_w} \\ \hline \mathbf{G_x}^\intercal & \mathbf{G_w}^\intercal & \mathbf{J_y} \end{array}\right)}_{\mathbf{J}} \cdot \underbrace{\left(\begin{array}{c} \nabla\mathrm{H}(\mathbf{x}) \\ \hline \mathbf{z}(\mathbf{w}) \\ \hline \mathbf{u} \end{array}\right)}_{\mathbf{b}}, \quad (2)$$

where matrices $\mathbf{J_x}$, $\mathbf{J_w}$ and $\mathbf{J_y}$ are skew-symmetric ($\mathbf{J}^\intercal = -\mathbf{J}$), and $\nabla\mathrm{H} : \mathbb{R}^s \to \mathbb{R}^s$ denotes the gradient of the total energy (Hamiltonian) w.r.t. the vector of the states $\mathbf{x}$. The pH system (2) fulfills the definition of passivity (see *e.g.* [9]), according to the following property.

Property 2.1 (Power Balance)**.** *The variation of the total energy* $\mathtt{E} = \mathrm{H}\big(\mathbf{x}\big)$ *of a system governed by (2) is given by (1), with the total dissipated power* $\mathtt{D} = \mathbf{z}(\mathbf{w})^\intercal \cdot \mathbf{w} \geq 0$ *and the total incoming power on external ports* $\mathtt{S} = \mathbf{u}^\intercal \cdot \mathbf{y}$.

Proof. We have $\mathbf{b}^\intercal \cdot \mathbf{a} = \frac{\mathrm{dE}}{\mathrm{d}t} + \mathtt{D} - \mathtt{S}$. Now $\mathbf{b}^\intercal \cdot \mathbf{a} = \mathbf{b}^\intercal \cdot \mathbf{J} \cdot \mathbf{b} = 0$ since $\mathbf{J}$ is skew-symmetric. □

2.3. Example

Consider the forced mass-spring-damper system in figure 2, with $s = 2$, $d = 1$ and $p = 1$, described as follows. For the mass and the damper, quantities are defined as previously with $x_1 = m\frac{\mathrm{d}q}{\mathrm{d}t}$ and $\mathbf{w} = [\frac{\mathrm{d}q}{\mathrm{d}t}]$. For the (linear) spring k, the state and the positive definite function can be the elongation (here the position of the mass) $x_2 = q$ and $\mathrm{H}_2(q) = \frac{k}{2}q^2$ so that $\mathfrak{e}_k = \mathrm{H}'_2$ and $\mathfrak{f}_k = \frac{\mathrm{d}x_2}{\mathrm{d}t}$. Port variables are arranged as input $\mathbf{u} = [\mathfrak{e}_{\text{ext}}]$ (applied force) and output $\mathbf{y} = [\mathfrak{f}_{\text{ext}}]$. Applying Newton's second law to this simple system yields

$$\left(\begin{array}{c} \mathfrak{e}_m \\ \hline \mathfrak{f}_k \\ \hline \mathfrak{f}_\alpha \\ \hline -\mathfrak{f}_{\text{ext}} \end{array}\right) = \left(\begin{array}{cc|c|c} 0 & -1 & -1 & +1 \\ \hline +1 & 0 & 0 & 0 \\ \hline +1 & 0 & 0 & 0 \\ \hline -1 & 0 & 0 & 0 \end{array}\right) \cdot \left(\begin{array}{c} \mathfrak{f}_m \\ \hline \mathfrak{e}_k \\ \hline \mathfrak{e}_\alpha \\ \hline -\mathfrak{e}_{\text{ext}} \end{array}\right).$$

From the constitutive laws of components, this equation exactly restores the form (2), block by block.

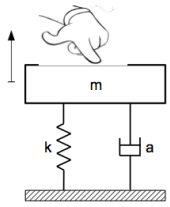

Figure 2: Damped harmonic oscillator with excitation.

3. LUMPED PARAMETERS COMPONENTS

In this this section, the standard modeling of the hammer and the pickup are recast as elementary port-Hamiltonian systems. Those systems are used in section 5 to form the global pH system.

3.1. Hammer $\mathcal{H}$

Here, we consider the standard piano hammer modeling, as depicted in [10, 11, 12]. It is composed of a simple mass with nonlinear spring and hysteresis effects due to the shape memory of the felt [13, 14, 2]. The actuation of the hammer is modeled as a simple force applied on the equivalent mass according to [15]. Denoting by q_h the position of the center of gravity, and m_h the total mass leads to the following dynamics [2]:

$$m_h\partial_t^2 q_h = -f_k(c) - f_\alpha(c) + f_h \quad (3)$$

where c is the crush of the felt, $f_k(c) = k_h c^\beta$ is the nonlinear spring effect, $f_\alpha(c) = \alpha_h \frac{\mathrm{d}(c^\beta)}{\mathrm{d}t}$ models the hysteresis effect and f_h is an external force. The contact with the beam is distributed according to $\omega(z) = 1(z - z_h)_{[-a_h/2, +a_h/2]}$, denoting by $z \in [0, l_b]$ the spacial coordinate along the beam with length l_b, and z_h and a_h respectively the position and width of the hammer [2]. The crush is $c = \lfloor l_h + q_h - \widehat{q}_b \rfloor_0$ with l_h the distance between the top of the felt at rest and q_h, $\lfloor x \rfloor_0$ the max of x and 0, and $\widehat{q}_b = \int_0^{l_b} q(z)\omega(z)\mathrm{d}z$ the weighted average of the beam's transverse displacement $q(z,t)$ (detailed in section 4). The pH model of the hammer (for instance disconnected from the beam) is derived as in example 2.3, and reads as follows.

Port-Hamiltonian modeling of the hammer $\mathcal{H}$

$$\mathbf{x}_\mathcal{H} = (m_h \tfrac{\mathrm{d}q_h}{\mathrm{d}t}, c)^\intercal,$$
$$\mathrm{H}_\mathcal{H}(\mathbf{x}_\mathcal{H}) = \tfrac{1}{2m_h}[\mathbf{x}_\mathcal{H}]_1^2 + \tfrac{k_h}{(\beta+1)}\lfloor [\mathbf{x}_\mathcal{H}]_2 + l_h \rfloor_0^{\beta+1}$$
$$\mathbf{w}_\mathcal{H} = \tfrac{\mathrm{d}c}{\mathrm{d}t}, \mathbf{z}_\mathcal{H}(\mathbf{w}_\mathcal{H}, \mathbf{x}_\mathcal{H}) = \tfrac{\alpha_h}{\beta}\lfloor [\mathbf{x}_\mathcal{H}]_2 + l_h \rfloor_0^{\beta-1}\mathbf{w}_\mathcal{H}$$
$$\mathbf{u}_\mathcal{H} = f_h, \quad \mathbf{y}_\mathcal{H} = \tfrac{\mathrm{d}q_h}{\mathrm{d}t}$$
$$\mathbf{J}_\mathbf{x} = \begin{pmatrix} 0 & -1 \\ 1 & 0 \end{pmatrix}, \mathbf{K} = \begin{pmatrix} 1 \\ 0 \end{pmatrix}, \mathbf{G}_\mathbf{x} = \begin{pmatrix} 1 \\ 0 \end{pmatrix}$$
$$\mathbf{J}_\mathbf{w} = 0, \mathbf{G}_\mathbf{w} = 0, \mathbf{J}_\mathbf{y} = 0$$

3.2. Pickup $\mathcal{P}$

Several arrangement of physically inspired signal processing modules to recover the nonlinear behavior of electric guitar pickups are available (see *e.g* [16, 17]). Here we consider the physical modeling approach of [18, 19]. According to the gyrator-capacitor approach [20, 21], we adopt the magnetic flux variation $\frac{\mathrm{d}\phi}{\mathrm{d}t}$ and the magnetomotive force h as magnetic power variables $\frac{\mathrm{d}\phi}{\mathrm{d}t}h = \mathtt{P}$. The magnet produces a constant magnetic field $h_0 = \frac{b_0}{\mu_0}$ which penetrates and magnetizes the beam (made of ferromagnetic material). This leads to consider in first approximation the beam as a magnetic dipole with constant amplitude. The flux ϕ_c of the total magnetic field in the coil is then the sum of the flux from the magnet $\phi_0 = a_c\mu_0 h_0$ and the flux from the magnetized beam which depends on the distance with the coil (of cross section a_c). Here, we consider a single vertical polarization of the beam, and the model in [19] reads:

$$\phi_c = \left(a_c + \frac{\Delta_\mu a_b}{(q_p(z_p) + l_p)^2}\right)\phi_0 \tag{4}$$

where $\Delta_\mu = \frac{\mu_\mathrm{rel}-1}{\mu_\mathrm{rel}+1}$, l_p is the distance from the beam at rest, q_p the vertical displacement of the beam measured at point z_p, and a_b is the section area of the beam. Thus, the magnet acts as a conservative gyrator modulated by the beam movement:

$$\begin{pmatrix} \frac{\mathrm{d}\phi_c}{\mathrm{d}t} \\ h_c \end{pmatrix} = \begin{pmatrix} 0 & f_p \\ \frac{1}{f_p} & 0 \end{pmatrix}\begin{pmatrix} \frac{\mathrm{d}\phi_0}{\mathrm{d}t} \\ h_0 \end{pmatrix}. \tag{5}$$

with $(\frac{\mathrm{d}\phi_c}{\mathrm{d}t}, h_c)$ the power variables associated to the ferromagnetic core of the coil, $q(z_p)$ the displacement of the beam measured at the pick-up position z_p, l_p the distance between the pickup and the beam at rest, $k_p = 2\Delta_\mu a_b a_c \mu_0$ and

$$f_p\left(q(z_p,t), \frac{\mathrm{d}q(z_p,t)}{\mathrm{d}t}\right) = \frac{k_p}{(q(z_p,t)+l_p)^3}\frac{\mathrm{d}q(z_p,t)}{\mathrm{d}t}. \tag{6}$$

From Ampere's theorem and Faraday's law, the coil is a constant magneto-electric gyrator [20, 21]:

$$\begin{pmatrix} v_c \\ i_c \end{pmatrix} = \begin{pmatrix} 0 & N \\ \frac{1}{N} & 0 \end{pmatrix}\begin{pmatrix} \frac{\mathrm{d}\phi_c}{\mathrm{d}t} \\ h_c \end{pmatrix}. \tag{7}$$

with N the number of wire turns and (v_c, i_c) the tension and current in the coil. Thus, the pickup acts as a modulated voltage source to the electronic circuit. Here we consider a simple RLC circuit, as shown in figure 3, with a high resistive load as mentioned in [18] so that the input current is $i_0 = 0$. Finally the port-Hamiltonian model of the pick-up is made of a two storage components (inductance and capacitance, with magnetic flux ϕ_L and charge q_C as respective states), a single dissipative component (resistance of the wire) and two ports (constant magnetomotive force and input current), as detailed below and in figure 3.

Port-Hamiltonian modeling of the pick-up $\mathcal{P}$

$$\mathbf{x}_\mathcal{P} = (\phi_L, q_C)^\intercal, \ \mathrm{H}_\mathcal{P}(\mathbf{x}_\mathcal{P}) = \tfrac{1}{2L_p}[\mathbf{x}_\mathcal{P}]_1^2 + \tfrac{1}{2C_p}[\mathbf{x}_\mathcal{P}]_2^2$$
$$\mathbf{w}_\mathcal{P} = i_r, \quad \mathbf{z}_\mathcal{P}(\mathbf{w}_\mathcal{P}) = r_p i_r$$
$$\mathbf{u}_\mathcal{P} = (h_0, i_0)^\intercal, \quad \mathbf{y}_\mathcal{P} = (\tfrac{\mathrm{d}\phi_0}{\mathrm{d}t}, v_0)^\intercal$$
$$\mathbf{J}_\mathbf{x} = \begin{pmatrix} 0 & -1 \\ 1 & 0 \end{pmatrix}, \mathbf{K} = \begin{pmatrix} 1 \\ 0 \end{pmatrix}, \mathbf{G}_\mathbf{x} = \begin{pmatrix} Nf_p & 0 \\ 0 & 1 \end{pmatrix}$$
$$\mathbf{J}_\mathbf{w} = 0, \mathbf{G}_\mathbf{w} = \mathbb{0}, \mathbf{J}_\mathbf{y} = \mathbb{0}$$

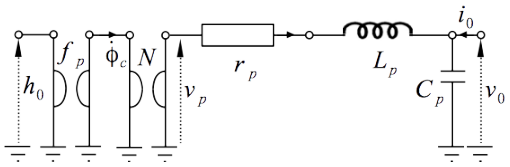

Figure 3: Schematic of the pick-up, where the voltage due to the beam movement is $v_p = Nf_p h_0$ with f_p as in equation (6).

4. BEAM $\mathcal{B}$

Here, we shall model the beam $\mathcal{B}$ in the port-Hamiltonian framework. We use the Euler-Bernoulli modeling of cantilever beam with damping, which results in a linear partial-differential equation. Although infinite dimensional systems perfectly fit in the pH framework (see [22, 23]), we firstly apply a standard modal decomposition and recast the resulting set of ordinary differential equations as a finite dimensional pH system.

4.1. Euler-Bernoulli modeling

The Euler-Bernoulli modeling of damped beam deflect $q(z,t)$ is

$$\rho\partial_t^2 q + \alpha\partial_t q + \kappa\partial_z^4 q = f \tag{8}$$

with initial conditions $q(z,0) = \frac{\mathrm{d}q}{\mathrm{d}t}(z,0) = 0$, and the following boundary conditions: no displacement at the base (bc1) $q(0,t) = 0$, no bending at the base (bc2) $\partial_z q(0,t) = 0$, no bending moment at the free end (bc3) $\partial_z^2 q(1,t) = 0$, no shearing force acting at the free end (bc4) $\partial_z^3 q(1,t) = 0$. ρ is a mass, κ is a stiffness and α is a fluid-like damping, each defined per unit length. Note the total internal energy is given by [24]:

$$\mathtt{E}_\mathcal{B} = \frac{1}{2}\int_0^{l_b}\left(\kappa\left(\partial_z^2 q\right)^2 + \rho\left(\frac{\mathrm{d}q}{\mathrm{d}t}\right)^2\right)\mathrm{d}z. \tag{9}$$

4.2. Finite dimensional approximation

The linear boundary value problem (8) admits an orthogonal basis of eigenfunctions $\mathcal{B} = \{\psi_m\}_{m\in\mathbb{N}_*}$ on the Hilbert space $L^2(0, l_b)$. Functions ψ_m which define the spacial modes are given in appendix 11 and shown in figure 4.

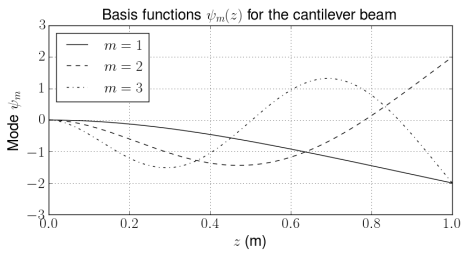

Figure 4: Eigenvectors of the Euler-Bernoulli cantilever beam.

Namely, they satisfy: (i) the boundary conditions (bc1-4); (ii) $\partial_z^4\psi(z) = k^4\psi(z)$; (iii) for all $(m,p) \in \mathbb{N}_*^2$, $\langle \psi_m, \psi_p \rangle = \delta_{m,p}$ (Kronecker's symbol) where the scalar product on $L^2(0,l_b)$ is defined by $\langle f,g\rangle = \int_0^{l_b} f(z)g(z)\mathtt{d}z$. This corresponds to select the modes k_m according to $\cos k_m l_b = \frac{-1}{\cosh k_m l_b}$, (see figure 5).

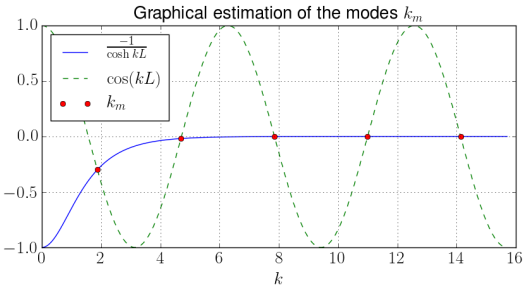

Figure 5: Graphical determination of the k_m.

We define $f = F^\intercal\Psi$, where $\Psi = (\psi_1,\dots,\psi_M)^\intercal$ is the vector of eigenmodes so that $F = (F_1,\dots,F_M)^\intercal = \langle f,\Psi\rangle$ is the projection of f on Ψ, and $\mathbf{q}_\mathcal{B} = \langle q,\Psi\rangle$. The relations satisfied by the $\mathbf{q}_\mathcal{B}$ are obtained by projecting equation (8) on base $\mathcal{B}$. This yields the following ordinary differential equations:

$$\rho\frac{\mathtt{d}^2\mathbf{q}_\mathcal{B}}{\mathtt{d}t^2} + \alpha\frac{\mathtt{d}\mathbf{q}_\mathcal{B}}{\mathtt{d}t} + \kappa\mathbf{L}\mathbf{q}_\mathcal{B} = F, \tag{10}$$

with $\mathbf{L} = \mathrm{diag}(k_1^4,\dots,k_M^4)$ which rewrites $\frac{\mathtt{d}\mathbf{x}_\mathcal{B}}{\mathtt{d}t} = \mathbf{A}\mathbf{x}_\mathcal{B} + \mathbf{B}\mathbf{u}_\mathcal{B}$ with $\mathbf{x}_\mathcal{B} = \left(\mathbf{q}_\mathcal{B}, \rho\frac{\mathtt{d}\mathbf{q}_\mathcal{B}}{\mathtt{d}t}\right)^\intercal$, $\mathbf{B} = (\mathbb{0},\mathbf{I_d})^\intercal$, $\mathbf{u}_\mathcal{B} = F$ and

$$\mathbf{A} = \begin{pmatrix} \mathbb{0} & \frac{1}{\rho}\mathbf{I_d} \\ -\kappa\mathbf{L} & -\frac{\alpha}{\rho}\mathbf{I_d} \end{pmatrix}$$

where $\mathbb{0}$ is the null matrix and $\mathbf{I_d}$ is the identity matrix. Note the transverse velocity is given by $\frac{\mathtt{d}q(z,t)}{\mathtt{d}t} = v(z,t) = \mathbf{v}(\mathbf{t})^\intercal\mathbf{\Psi}(\mathbf{z})$ with $\mathbf{v}(\mathbf{t}) = \mathbf{B}^\intercal\frac{1}{\rho}\mathbf{x}_\mathcal{B}(\mathbf{t})$.

4.3. Port-Hamiltonian formulation

From (9) and the modal reconstruction $q = \mathbf{q}_\mathcal{B}^\intercal\Psi$, the total energy of the beam is the Hamiltonian $\mathrm{H}_\mathcal{B}(\mathbf{x}_\mathcal{B}) = \frac{1}{2}\mathbf{x}_\mathcal{B}^T\mathbf{W}\mathbf{x}_\mathcal{B}$, with

$$\mathbf{W} = \begin{pmatrix} \kappa\mathbf{L} & \mathbb{0} \\ \mathbb{0} & \rho^{-1}\mathbf{I_d} \end{pmatrix},$$

since $\langle \partial_z^2\Psi, \partial_z^2\Psi^\intercal\rangle = \mathbf{L}$. The output is $\mathbf{y}_\mathcal{B} = \mathbf{B}^\intercal\nabla\mathrm{H}_\mathcal{B} = \frac{\mathtt{d}\mathbf{q}_\mathcal{B}}{\mathtt{d}t}$ so that the incoming power is $\mathtt{P} = \mathbf{y}_\mathcal{B}^\intercal\mathbf{u}_\mathcal{B} = \int_0^{l_b}\mathbf{y}_\mathcal{B}^\intercal\Psi\Psi^T\mathbf{u}_\mathcal{B}\mathtt{d}z$ (with $\mathbf{u}_\mathcal{B} = F$). The resulting port-Hamiltonian system is given below.

Port-Hamiltonian modeling of the beam $\mathcal{B}$

$$\mathbf{x}_\mathcal{B} = \left(\mathbf{q}_\mathcal{B}, \rho\tfrac{\mathtt{d}\mathbf{q}_\mathcal{B}}{\mathtt{d}t}\right)^\intercal, \quad \mathrm{H}_\mathcal{B}(\mathbf{x}_\mathcal{B}) = \tfrac{1}{2}\mathbf{x}_\mathcal{B}^\intercal\mathbf{W}\mathbf{x}_\mathcal{B}$$
$$\mathbf{w}_\mathcal{B} = \tfrac{\mathtt{d}\mathbf{q}_\mathcal{B}}{\mathtt{d}t}, \quad \mathbf{z}_\mathcal{B}(\mathbf{w}_\mathcal{B}) = \alpha\mathbf{w}_\mathcal{B}$$
$$\mathbf{u}_\mathcal{B} = F = \langle f,\Psi\rangle, \quad \mathbf{y}_\mathcal{B} = \tfrac{\mathtt{d}\mathbf{q}_\mathcal{B}}{\mathtt{d}t}$$
$$\mathbf{J_x} = \begin{pmatrix} \mathbb{0} & \mathbf{I_d} \\ -\mathbf{I_d} & \mathbb{0} \end{pmatrix}, \mathbf{K} = \begin{pmatrix} \mathbb{0} \\ \mathbf{I_d} \end{pmatrix}, \mathbf{G_x} = \begin{pmatrix} \mathbb{0} \\ \mathbf{I_d} \end{pmatrix}$$
$$\mathbf{J_w} = \mathbb{0}, \mathbf{G_w} = \mathbb{0}, \mathbf{J_y} = \mathbb{0}$$

5. INTERCONNECTION

In this section we derive the global port-Hamiltonian modeling of the system $(\mathcal{H},\mathcal{B},\mathcal{P})$ from the interconnection of the elementary pH systems derived in sections 3 and 4. First we connect the mechanical components $(\mathcal{H},\mathcal{B})$ and second the pick-up which is not energetically but geometrically coupled to the former part.

The connection of two pH systems is again a pH system (see [25]). The state $\mathbf{x}$, the dissipative variable $\mathbf{w}$ and dissipative functions $\mathbf{z}$ are obtained by concatenating the subsystems, and the Hamiltonian is the sum of the local Hamiltonians.

5.1. Mechanical part

The input of the pH system that models the beam is the projection of the applied force $f(z,t)$ on the modal basis $\Psi(z)$. When interconnected with the hammer, this is given by the force due to the felt compression $f_k + f_\alpha$ distributed according to $\omega(z)$ (see section 3.1): $\mathbf{u}_\mathcal{B} = F = \Omega f_\mathcal{H}$ with $\Omega = \langle\omega,\Psi\rangle$. Correspondingly, the variation of the felt's crush is computed from the averaged velocity of the beam. This interconnection results in a single-input/single-output pH system (the input being the force applied to the hammer).

5.2. Complete port-Hamiltonian modeling

Finally, we include the modeling of the pickup and analog circuit. As already stated, the mechanical part is not energetically coupled to the electromagnetic part, and the complete modeling is obtained by concatenating the interconnection $(\mathcal{H},\mathcal{B})$ with the pickup $\mathcal{P}$. This yields the following pH system.

Port-Hamiltonian modeling of the system $\mathcal{H}+\mathcal{B}+\mathcal{P}$

$$\mathbf{x} = (\mathbf{x}_\mathcal{H},\mathbf{x}_\mathcal{B},\mathbf{x}_\mathcal{P})^\intercal, \ \mathrm{H}(\mathbf{x}) = \mathrm{H}_\mathcal{H}(\mathbf{x}_\mathcal{H}) + \mathrm{H}_\mathcal{B}(\mathbf{x}_\mathcal{B}) + \mathrm{H}_\mathcal{P}(\mathbf{x}_\mathcal{P})$$
$$\mathbf{w} = (\mathbf{w}_\mathcal{H},\mathbf{w}_\mathcal{B},\mathbf{w}_\mathcal{P})^\intercal, \ \mathbf{z}(\mathbf{w}) = \left(\mathbf{z}_\mathcal{H}(\mathbf{w}_\mathcal{H}),\mathbf{z}_\mathcal{B}(\mathbf{w}_\mathcal{B}),\mathbf{z}_\mathcal{P}(\mathbf{w}_\mathcal{P})\right)^\intercal$$
$$\mathbf{u} = (f_h,h_0,i_0)^\intercal, \quad \mathbf{y} = (\tfrac{\mathtt{d}q_h}{\mathtt{d}t},\tfrac{\mathtt{d}\phi_0}{\mathtt{d}t},v_0)^\intercal$$
$$\mathbf{J_x} = \begin{pmatrix} 0 & -1 & \mathbb{0} & \mathbb{0} & 0 & 0 \\ 1 & \mathbb{0} & \mathbb{0} & -\Omega^\intercal & 0 & 0 \\ \mathbb{0} & \mathbb{0} & \mathbb{0} & \mathbf{I_d} & \mathbb{0} & \mathbb{0} \\ \mathbb{0} & \Omega & -\mathbf{I_d} & \mathbb{0} & \mathbb{0} & \mathbb{0} \\ 0 & 0 & \mathbb{0} & \mathbb{0} & 0 & -1 \\ 0 & 0 & \mathbb{0} & \mathbb{0} & 1 & 0 \end{pmatrix},$$
$$\mathbf{K} = \begin{pmatrix} 1 & \mathbb{0} & 0 \\ 0 & \mathbb{0} & 0 \\ \mathbb{0} & \mathbb{0} & \mathbb{0} \\ -\Omega & \mathbf{I_d} & \mathbb{0} \\ 0 & \mathbb{0} & 1 \\ 0 & \mathbb{0} & 0 \end{pmatrix}, \mathbf{G_x} = \begin{pmatrix} 1 & 0 & 0 \\ 0 & 0 & 0 \\ \mathbb{0} & \mathbb{0} & \mathbb{0} \\ \mathbb{0} & \mathbb{0} & \mathbb{0} \\ 0 & Nf_\mathcal{P} & 0 \\ 0 & \mathbb{0} & 1 \end{pmatrix}$$
$$\mathbf{J_w} = \mathbb{0}, \mathbf{G_w} = \mathbb{0}, \mathbf{J_y} = 0$$

6. NUMERICAL SCHEME

To ensure stable simulation of stable dynamical system $\frac{\mathtt{d}\mathbf{x}}{\mathtt{d}t} = \mathbf{f}(\mathbf{x})$, many numerical schemes focus on the approximation quality of the time derivative, combined with operation of the vector field $\mathbf{f}$. Here, we adopt an alternative point of view, by transposing the power balance (1) in the discrete time-domain to preserve passivity. This is achieved by numerical schemes that provide a discrete version of the chain rule for computing the derivative of $\mathtt{E} = \mathrm{H}\circ\mathbf{x}$. This is the case of Euler scheme, for which first order approximation of the differential applications $\mathtt{d}\mathbf{x}(t,\mathtt{d}t) = \frac{\mathtt{d}\mathbf{x}}{\mathtt{d}t}(t)\cdot\mathtt{d}t$ and

$\mathtt{dH}(\mathbf{x},\mathbf{dx}) = \nabla \mathrm{H}(\mathbf{x})^\intercal \cdot \mathbf{dx}$ on the sample grid $t \equiv kT,\ k \in \mathbb{Z}$ are given by

$$\begin{aligned} \delta\mathbf{x}(k,T) &= \mathbf{x}(k+1) - \mathbf{x}(k), && (11)\\ \delta \mathrm{H}\big(\mathbf{x},\delta\mathbf{x}\big) &= \mathrm{H}\big(\mathbf{x}+\delta\mathbf{x}\big) - \mathrm{H}\big(\mathbf{x}\big) && (12)\\ &= \nabla_d \mathrm{H}\big(\mathbf{x},\mathbf{x}+\delta\mathbf{x}\big)^\intercal \cdot \delta\mathbf{x}. \end{aligned}$$

For mono-variate storage components ($\mathrm{H}(\mathbf{x}) = \sum_{n=1}^{s} \mathrm{H}_n(x_n)$), the solution can be built element-wise with the n-th coordinate given by

$$[\nabla_d \mathrm{H}\big(\mathbf{x},\mathbf{x}+\delta\mathbf{x}\big)]_n = \begin{cases} \frac{h_n\left(x_n+\delta x_n\right) - h_n\left(x_n\right)}{\delta x_n} & \text{if } \delta x_n \neq 0,\\ h_n'(x_n) & \text{otherwise.} \end{cases} \quad (13)$$

A discrete chain rule is indeed recovered

$$\frac{\delta \mathtt{E}(k,T)}{T} = \nabla_d \mathrm{H}\big(\mathbf{x}(k),\mathbf{x}(k+1)\big)^\intercal \cdot \frac{\delta\mathbf{x}(k,T)}{T} \quad (14)$$

so that the following substitution in (2)

$$\begin{array}{rcl} \frac{\mathbf{dx}}{\mathbf{dt}}(t) & \rightarrow & \frac{\delta\mathbf{x}(k,T)}{T}\\ \nabla \mathrm{H}(\mathbf{x}) & \rightarrow & \nabla_d \mathrm{H}\big(\mathbf{x}(k),\mathbf{x}(k+1)\big) \end{array} \quad (15)$$

leads to

$$\begin{aligned} 0 &= \mathbf{b}(k)^\intercal \cdot \mathbf{J} \cdot \mathbf{b}(k) = \mathbf{b}(k)^\intercal \cdot \mathbf{a}(k)\\ &= \underbrace{\left[\nabla_d \mathrm{H}^\intercal \cdot \frac{\delta\mathbf{x}}{\delta t}\right](k)}_{\frac{\delta \mathtt{E}(k,T)}{T}} + \underbrace{\mathbf{z}(\mathbf{w}(k))^\intercal \cdot \mathbf{w}(k)}_{\mathtt{D}(k)} - \underbrace{\mathbf{u}(k)^\intercal \cdot \mathbf{y}(k)}_{\mathtt{S}(k)}. \end{aligned} \quad (16)$$

For pH systems composed of a collection of linear energy storing components with quadratic Hamiltonian $\mathrm{H}_n(x_n) = \frac{x_n^2}{2C_n}$, we define $\mathbf{Q} = \mathrm{diag}(C_1 \cdots C_s)^{-1}$ so that the discrete gradient (13) reads

$$\nabla_d \mathrm{H}\big(\mathbf{x},\mathbf{x}+\delta\mathbf{x}\big) = \mathbf{Q}\left(\mathbf{x}(k) + \tfrac{\delta\mathbf{x}(k)}{2}\right), \quad (17)$$

which restores the midpoint rule. For nonlinear case, (13) leads to another numerical scheme depending on the nonlinearity, still preserving passivity.

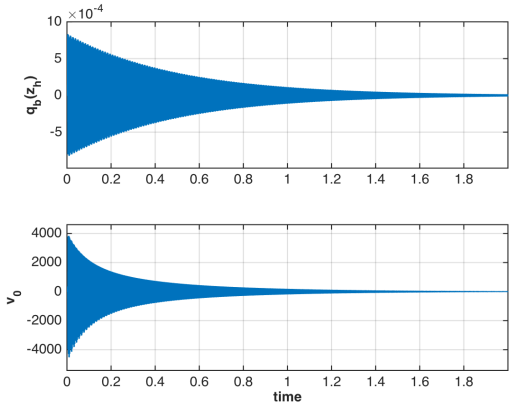

Figure 6: Temporal evolution of the beam displacement measured at pickup position $q(z_h)$ and output voltage v_0 ($f_h = 2000N$).

7. SIMULATION RESULTS

In this section, the numerical scheme (15) is applied on the modeling presented in section 5. First, we discuss the physical parameters used for the simulation. Second, results are shown.

7.1. Physical parameters

The sample rate is 48kHz. The parameters of the hammer are [2]: $m_h = 5\text{g}$, $\beta = 2$, $k_h = 10^6\text{N.m}^{-1}$, $a_h = 1\text{cm}$, $z_h = 2.35\text{cm}$, $\alpha_h = 0.1\text{N.s.m}^{-1}$ and $l_h = 1$. It is supposed initially at rest, 20cm below the beam. The force on the hammer is $f_h = 200\text{N}$ and then 2000N, during 1ms. For a cylindrical bream with radius $r = 2\text{mm}$ made of steel, the mass and stiffness per unit length are respectively $\rho = \varrho\pi r^2\text{kg.m}^{-1}$ and $\kappa = E_s\frac{\pi r^4}{4}$, with $\varrho = 7750\text{kg.m}^{-3}$ the density and $E_s = 180.10^9\text{N.m}^{-2}$ the young modulus of steel. The length l_b is chosen so that the frequency of the first mode (without damping) corresponds to the desired tone, here 440Hz, which yields $l_b = 7.83\text{cm}$. The pickup is supposed to be positioned $l_p = 1\text{mm}$ below the beam, at $z_h = 6.26\text{cm}$, and we set arbitrarily $Nk_ph_0 = 10^-6$. The cutoff frequency of the RLC circuit is 500Hz, with $C_p = 330\text{nF}$, $L_p = 307\text{mH}$ and $r_p = 1\text{k}\Omega$.

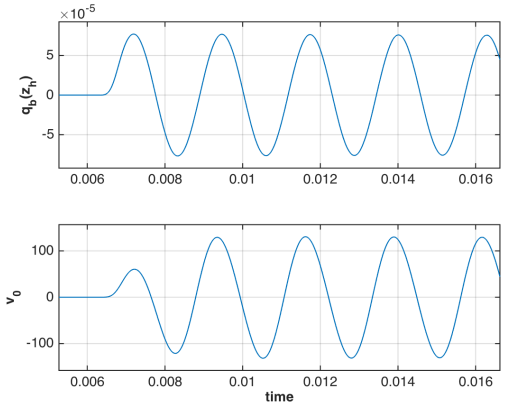

(a) $f_h = 200N$.

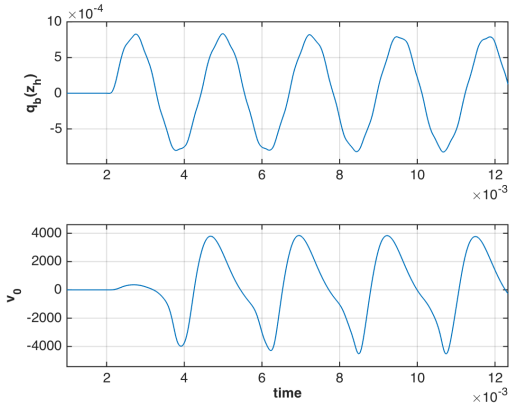

(b) $f_h = 2000N$.

Figure 7: Zoom on the beam displacement measured at pickup position $q(z_h)$ and output voltage v_0.

7.2. Waveforms

The waveform associated to the beam displacement measured at pickup position $q(z_h)$ and the output voltage v_0 are shown in figures 6. The force applied on the hammer is (i) $f_h = 200$N (figure 7a) and (ii) $f_h = 2000$N (figures 6 and 7b), during 1ms. In case (i), the beam's displacement measured by the pickup $q(z_h)$ corresponds to 6% of the distance pickup-beam l_p, which coincide with the linear behavior. In case (ii), $q(z_h) \simeq 70\% l_p$, which causes the observed change in the waveform.

7.3. Mechanical energy

The dynamics of the hammer is shown in figure 8a for the case (ii) ($f_h = 2000$N). We see it accelerates between 1ms and 2ms and impacts the beam at $t_i \simeq 2.5$ms. During the impact, a part of the energy transferred from the hammer to the beam is dissipated in the later (see figure 8b). The energy in the beam is shown in figure 9. We see the numerical error on the power balance is close to the machine epsilon.

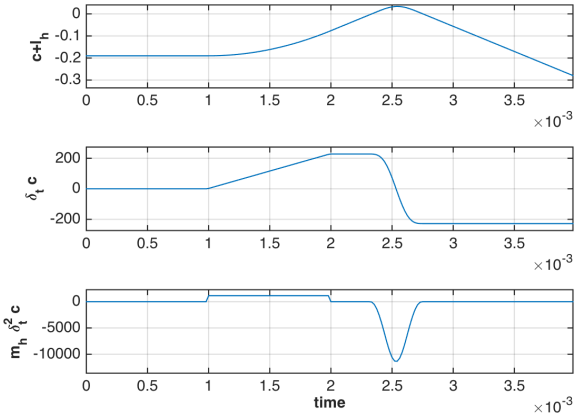

(a) Position, velocity and inertial force of the hammer.

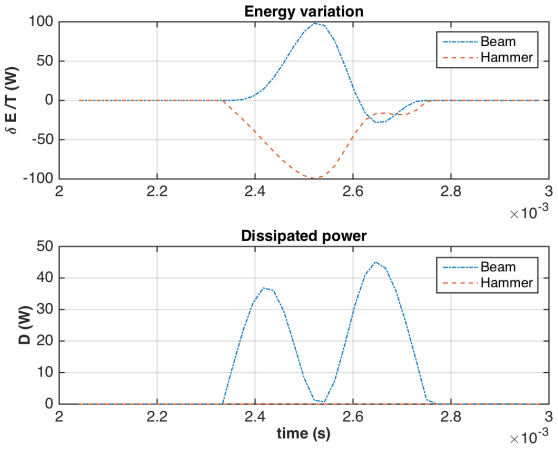

(b) Energy transfer between the hammer and the beam.

Figure 8: Impact hammer $\mathcal{H}$ - beam $\mathcal{B}$

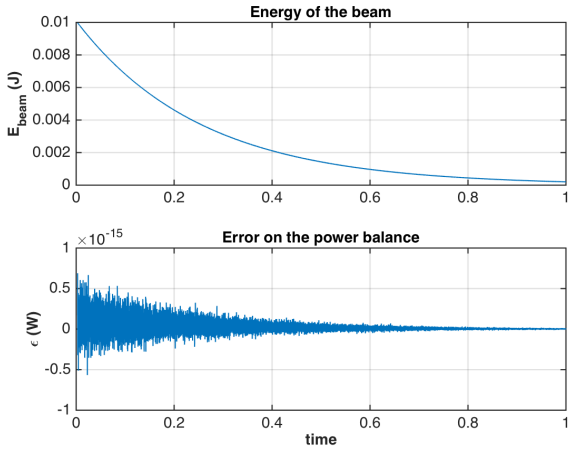

Figure 9: Mechanical energy and error on the power balance $\epsilon = \frac{\delta \mathrm{E}_{beam}}{T} + \mathrm{D}_{beam}$.

7.4. Electromagnetic energy

The source of magnetomotive force is modulated according to section 3.2, which can me modeled as a voltage source (with arbitrary amplitude since the output RLC circuit is linear). Note such a source can be locally a sink of power, as seen in figure 10 where the power of the source pass slightly under 0. Again, the numerical error on the power balance is close to the machine epsilon (figure 11).

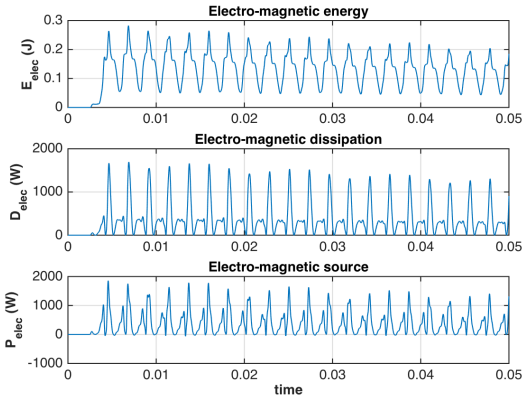

Figure 10: Energy, power dissipation and source of the electro-magnetic part.

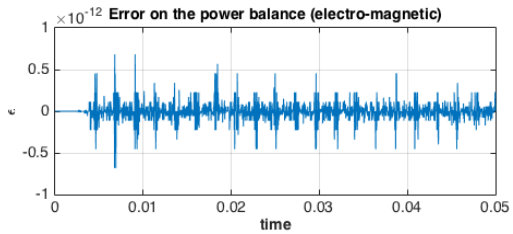

Figure 11: Error on the electro-magnetic power balance.

8. CONCLUSIONS

In this paper, a nonlinear finite-dimensional model of a simplified electro-mechanical piano has been developed, based on a set of elementary components (hammer, beam and pickup), in the framework of port Hamiltonian systems. This formalism decomposes the system into conservative, dissipative and source parts. A numerical method has been derived, which preserves this decomposition and the power balance in the discrete time domain. The analysis of numerical results proves the relevancy of the method: first, the nonlinearity provides an sound enrichment with the force of the hammer; second, the analysis of the power exchanges and of the total energy shows that passivity is fulfilled.

A perspective of this work is to refine the modeling of the mechano-electric transducer. First, the pickup could be placed in the axis of the beam, as in the case of the Fender Rhodes piano. Second, the modeling should include the energetic exchange due to the coupling between the beam and the magnet, by considering the Maxwell force. Another perspective is to estimate the physical parameters from a real device to increase the sound realism. Finally, second order explicit numerical schemes (see *e.g.* [26]) could be examined to improve accuracy and reduces the computational cost.

9. ACKNOWLEDGMENTS

The authors acknowledge the members of the french national research agency project HaMecMoPSys for support in port-Hamiltonian theory, and Cyril Touzé for lectures on modal decomposition.

10. REFERENCES

[1] Stefan Bilbao, Alberto Torin, and Vasileios Chatziioannou, "Numerical modeling of collisions in musical instruments," *Acta Acustica united with Acustica*, vol. 101, no. 1, pp. 155–173, 2015.

[2] Juliette Chabassier, Antoine Chaigne, and Patrick Joly, "Modeling and simulation of a grand piano," *The Journal of the Acoustical Society of America*, vol. 134, no. 1, pp. 648–665, 2013.

[3] Gianpaolo Borin, Davide Rocchesso, and Francesco Scalcon, "A physical piano model for music performance," in *Proceedings: International Computer Music Conference 1997, Thessaloniki, Hellas, 25-30 september 1997*. The International Computer Music Association, 1997, pp. 350–353.

[4] Balázs Bank, "Nonlinear interaction in the digital waveguide with the application to piano sound synthesis," in *Proc. International Computer Music Conference (ICMC'00)*, 2000, pp. 54–57.

[5] BM Maschke, Arjan J Van Der Schaft, and Peter C Breedveld, "An intrinsic hamiltonian formulation of network dynamics: Non-standard poisson structures and gyrators," *Journal of the Franklin institute*, vol. 329, no. 5, pp. 923–966, 1992.

[6] Arjan van der Schaft, "Port-hamiltonian systems: an introductory survey," in *Proceedings of the International Congress of Mathematicians Madrid, August 22–30, 2006*, 2007, pp. 1339–1365.

[7] Vincent Duindam, Alessandro Macchelli, Stefano Stramigioli, and Herman Bruyninckx, *Modeling and Control of Complex Physical Systems: The Port-Hamiltonian Approach*, Springer Science & Business Media, 2009.

[8] Jerrold E Marsden and Tudor Ratiu, *Introduction to mechanics and symmetry: a basic exposition of classical mechanical systems*, vol. 17, Springer Science & Business Media, 2013.

[9] Hassan K Khalil and JW Grizzle, *Nonlinear systems*, vol. 3, Prentice hall New Jersey, 1996.

[10] Neville Horner Fletcher and Thomas D Rossing, *The physics of musical instruments*, Springer Science & Business Media, 1998.

[11] Xavier Boutillon, "Model for piano hammers: Experimental determination and digital simulation," *The Journal of the Acoustical Society of America*, vol. 83, no. 2, pp. 746–754, 1988.

[12] N Giordano and JP Winans II, "Piano hammers and their force compression characteristics: Does a power law make sense?," *The Journal of the Acoustical Society of America*, vol. 107, no. 4, pp. 2248–2255, 2000.

[13] Anatoli Stulov, "Experimental and theoretical studies of piano hammer," in *Proceedings of the Stockholm Music Acoustics Conference*, 2003.

[14] Balázs Bank, Federico Avanzini, Gianpaolo Borin, Giovanni De Poli, Federico Fontana, and Davide Rocchesso, "Physically informed signal processing methods for piano sound synthesis: a research overview," *EURASIP Journal on Applied Signal Processing*, vol. 2003, pp. 941–952, 2003.

[15] Harry C Hart, Melville W Fuller, and Walter S Lusby, "A precision study of piano touch and tone," *The Journal of the Acoustical Society of America*, vol. 6, no. 2, pp. 80–94, 1934.

[16] Rafael CD Paiva, Jyri Pakarinen, and Vesa Välimäki, "Acoustics and modeling of pickups," *Journal of the Audio Engineering Society*, vol. 60, no. 10, pp. 768–782, 2012.

[17] Luca Remaggi, Leonardo Gabrielli, R Cauduro Dias de Paiva, Vesa Välimäki, and Stefano Squartini, "A pickup model for the clavinet," in *Digital Audio Effects Conference 2012 (DAFx-12)*, 2012.

[18] Nicholas G Horton and Thomas R Moore, "Modeling the magnetic pickup of an electric guitar," *American journal of physics*, vol. 77, no. 2, pp. 144–150, 2009.

[19] K. T. McDonald, "Electric guitar pickups," in *Pedagogic note*. May 2007, Princeton University, Department of Physics, `http://puhep1.princeton.edu/~mcdonald/examples/guitar.pdf`,.

[20] David C Hamill, "Lumped equivalent circuits of magnetic components: the gyrator-capacitor approach," *IEEE transactions on power electronics*, vol. 8, no. 2, pp. 97–103, 1993.

[21] David C Hamill, "Gyrator-capacitor modeling: a better way of understanding magnetic components," in *Applied Power Electronics Conference and Exposition, 1994. APEC'94. Conference Proceedings 1994., Ninth Annual*. IEEE, 1994, pp. 326–332.

[22] Alessandro Macchelli and Claudio Melchiorri, "Modeling and control of the timoshenko beam. the distributed port hamiltonian approach," *SIAM Journal on Control and Optimization*, vol. 43, no. 2, pp. 743–767, 2004.

[23] Javier Andres Villegas, *A port-Hamiltonian approach to distributed parameter systems*, Ph.D. thesis, 2007.

[24] Leonard Meirovitch, *Principles and techniques of vibrations*, vol. 1, Prentice Hall New Jersey, 1997.

[25] Joaquín Cervera, AJ Van Der Schaft, and Alfonso Baños, "Interconnection of port-hamiltonian systems and composition of dirac structures," *Automatica*, vol. 43, no. 2, pp. 212–225, 2007.

[26] Nicolas Lopes, Nicolas Hélie, and Antoine Falaize, "Explicit second-order accurate method for the passive guaranteed simu- lation of port-hamiltonian systems.," in *5th IFAC Workshop on Lagrangian and Hamiltonian Methods for Non Linear Control (Lyon, France)*, July 2015, Accepted.

11. APPENDIX: ORTHONORMAL BASIS

The linear boundary value problem (8) admits an orthogonal basis of eigenfunctions $\mathcal{B} = \{\psi_m\}_{m\in\mathbb{N}_*}$ on the Hilbert space $L^2(0, l_b)$, namely, the spacial modes $\psi_m(z)$ which satisfy: (i) the boundary conditions (bc1-4); (ii) $\partial_z^4\psi(z) = k^4\psi(z)$; (iii) for all $(m, p) \in \mathbb{N}_*^2$, $\langle\psi_m, \psi_p\rangle = \delta_{m,p}$ (Kronecker's symbol), where the scalar product on $L^2(0, l_b)$ is defined by $\langle f, g\rangle = \int_0^{l_b} f(z)g(z)\mathtt{d}z$. This corresponds to select the modes k_m according to $\cos k_m l_b = \frac{-1}{\cosh k_m l_b}$:

$$
\begin{aligned}
\psi_m(z) &= \gamma\widehat{\psi}_m(z)\\
\widehat{\psi}_m(z) &= \theta_m\left(\sin k_m z - \sinh k_m z\right) + \cos k_m z - \cosh k_m z\\
\theta_m &= \tfrac{\sin k_m l_b - \sinh k_m l_b}{\cos k_m l_b + \cosh k_m l_b}\\
\gamma &= \Bigg(\tfrac{k_m l_b(\cos 2k_m l_b + \cosh 2k_m l_b - 2)}{2k_m(\cos k_m l_b + \cosh k_m l_b)^2}\\
&\qquad \tfrac{\cosh k_m l_b(2\sin k_m l_b + \cosh k_m l_b \sin 2k_m l_b)}{2k_m(\cos k_m l_b + \cosh k_m l_b)^2}\Bigg)^{\frac{1}{2}}.
\end{aligned}
$$